Erciyes Üniversitesi
Fen Bilimleri Enstitüsü Dergisi
Cilt 41, Sayı 1, 2025

Erciyes University
Journal of Institue Of Science and Technology
Volume 41, Issue 1, 2025

Optimization of Emulsification Parameters for Chasteberry (*Vitex agnus-castus L.*) Essential Oil Aqueous Nanoemulsions

İlhan Özen*[1], Oğuz Demiryürek[1]

*[1]Department of Textile Engineering, Faculty of Engineering, Erciyes University, Melikgazi, Kayseri 38030, Türkiye

(Alınış / Received: 06.02.2025, Kabul / Accepted: 06.04.2025, Online Yayınlanma / Published Online: 30.04.2025)

Keywords
Chasteberry oil, Tween80, Ultrasonication, Nanoemulsion

Abstract: Chasteberry essential oil (CEO) is known as an efficient compound for women's health. However, in order to increase its efficacy, it should be preserved until use. One option for this purpose is to prepare its nanoemulsions. Here, feasibility of CEO nanoemulsion formulation development was reported without the need of co-surfactants and co-solvents employing a simple ultrasonication process, which was complemented by statistical evaluation. To that end, CEO NEs were prepared using an ultrasonic homogenizer using only water as the solvent and Tween80 (T80) as the emulsifier. Variations in the emulsification parameters such as emulsifier concentration (CEO/T80 ratio: 1/0, 1/1, 1/2, and 1/4) and ultrasonication time (0, 1, 5, 10, and 20 min) were tested. Turbidity measurements and morphology analyses were performed in addition to dynamic light scattering measurements. On the basis of statistical evaluation of droplet size and Zeta potential values, the best emulsification process parameters were revealed. The minimum droplet size (estimate: 37 nm) was achieved accompanying by a high Zeta potential value of -36 mV when employed an ultrasonication time of 10.55 min by using T1 (CEO/T80: 1/1). Morphology analyses delivered complementary results.

Hayıtotu (*Vitex agnus-castus L.*) Esansiyel Yağı Sulu Nanoemülsiyonları için Emülsifikasyon Parametrelerinin Optimizasyonu

Anahtar Kelimeler
Hayıtotu Yağı, Tween80, Ultrasonikasyon, Nanoemülsiyon

Öz: Hayıtotu esansiyel yağı (HEY) kadın sağlığı için etkili bir bileşen olarak bilinmektedir. Bununla beraber, etkinliğini arttırmak için HEY'in kullanıma kadar korunması gerekmektedir. Bu amaç için bir seçenek, HEY'in nanoemülsiyonlarını (NE) hazırlamaktır. Burada HEY NE formülasyonlarının basit bir ultrasonikasyonla yüzeyaktif madde ve yardımcı çözgen gereksinimi olmadan yapılabilirliği ve istatistiksel değerlendirmesi raporlanmıştır Bu amaçla HEY NE'ler çözgen olarak sadece su ve emülgatör olarak Tween80 (T80) kullanılarak ultrasonik homojenleştirici ile hazırlanmıştır. Emülgatör konsantrasyonu (HEY/T80 oranı: 1/0, 1/1, 1/2 ve 1/4) ve ultrasonikasyon süresi (0, 1, 5, 10, ve 20 dk.) gibi emülsifikasyon parametrelerindeki varyasyonlar test edilmiştir. Dinamik ışık saçılımı ölçümlerine ilaveten bulanıklık ölçümleri ve morfoloji analizleri gerçekleştirilmiştir. Damlacık boyutu ve Zeta potansiyeli verilerinin istatistiksel değerlendirmesine göre en iyi emülsifikasyon parametreleri ortaya çıkarılmıştır. T1 (HEY/T80: 1/1) kullanılarak 10.55 dk'lık ultrasonikasyon süresinde -36 mV'luk yüksek bir Zeta potansiyeli eşliğinde en küçük damlacık boyutunun (tahmin değeri: 37 nm) elde edilebileceği gösterilmiştir. Morfoloji analizleri tamamlayıcı sonuçlar vermiştir.

*İlgili Yazar, email: iozen@erciyes.edu.tr

1. Introduction

Essential oils, extracted from medicinal plants and containing a mixture of many bioactive compounds, have always been played a key role for keeping a healthy life [1]. However, they have some drawbacks such as water insolubility, unstability, and volatility, which should be overcome to fully exploit their potential in various fields [2,3]. Making emulsions is one of the easiest ways to improve their efficiency, in which essential oils are dispersed in a solvent (mostly water) as spherical droplets with the help of an emulsifier [4-6].

Emulsifiers are surface active molecules, which positions at the oil-water interface, reduces the interfacial tension, and hinders (or delays) the aggregation of droplets [7]. Typically, its hydrophilic part is in the aqueous phase, while the hydrophobic tail remains enclosed in the oil phase [8,9]. Emulsifiers are classified according to their hydrophilic-lipophilic balance (HLB) values. Water-in-oil (W/O) emulsions are produced using surfactants with a low HLB (3-6) value, while oil-in-water (O/W) emulsions are created with surfactants with a high HLB (8-15) value. Small-molecule non-ionic surfactants such as polyoxyethylene sorbitan fatty acid esters (tweens), sugar esters and monoglycerides are extensively used as emulsifiers [10-13].

Based on their droplet size and stability, there are 3 types of emulsions, i.e., coarse emulsions (1-100 μm), microemulsions (10-100 nm), and nanoemulsions (NE; 20-500 nm) [14-16]. Microemulsion forms spontaneously since its free energy is lower than its phase-separated components. They are optically transparent as the particle size is lesser than the wavelength (typically <100 nm) and weakly scatters light [14]. Nanoemulsions have droplet dimensions similar to the microemulsions ranging from <200 and in some cases <100 nm [17]. Nanoemulsions are not affected by physical and chemical variations including temperature and pH. They require less amount of surfactants for their preparation. Their stability and efficacy is more pronounced than microemulsions [18,19].

Nanoemulsions can be prepared by either bottom up or top-down approach, which are also known as low energy and high energy methods, respectively. In the low energy methods including spontaneous emulsification, emulsion-inversion point, phase-inversion composition, and phase-inversion temperature methods, NEs are prepared by altering the temperature or composition of the oil-water system and the energy input is from the chemical potential of the constituents [20]. The high energy methods involve the use of mechanical devices such as high-pressure homogenizer, micro-fluidizer, or ultrasonicator. Within high-energy methods, ultrasonicators have been the instrument of choice, since they feature advantages such as being easy to operate and clean. Their energy efficiency is high and they provide a good emulsion stability by using less amount of emulsifier [21,22]. Ultrasonicators transform energy into mechanical vibrations transmitted by a probe system, which is directly applied to the sample afterwards [23]. These physical effects disrupt droplets and facilitate the formation of stable O/W and/or W/O emulsions with small droplets size [24].

Chasteberry essential oil (CEO), extracted from *Vitex agnus-castus L.*, is widely used for the treatment of premenstrual syndrome (PMS), menstrual irregularities, fertility disorders, and symptoms of menopause [25]. In addition, CEO has antifungal property against Candida albicans fungus [26-28], being useful for treating itching/irritation in sensitive areas. Despite its well-known beneficial properties for women's health, CEO has been used only a few times in nanoemulsion formulation [29,30]. In the related studies, it is striking that many co-surfactants and co-solvents were employed. In addition, the NEs generated were not statistically evaluated. In our study, we showed for the first time that stable CEO NEs could be generated without the need of many chemicals and cumbersome processing steps. To that end, only water and only Tween80 were used. Tween80 has been chosen due to having an HLB value of 15 [31], which is suitable for preparing aqueous chasteberry oil O/W nanoemulsions. Droplet size and Zeta potential measurement results were statistically evaluated and optimum processing conditions were established.

2. Material and Method

2.1. Materials

Chasteberry essential oil (CEO) (100% pure steam-distilled extract of *Vitex agnus-castus L.*) was supplied by Ahimsa Oils, Australia. According to the manufacturer's declaration, the main components are 1,8-cineole (20.18%), sabinene (19.02%), α-pinene (15.73%), β-Caryophyllene (12.89%) and trans-β-farnesene (6.02%) [32]. Tween80 (T80) and all other chemicals and solvents were purchased from Sigma Aldrich Pty. Ltd, Australia. Ultrapure water (conductivity: 0.055 μS/cm) was used in all experiments.

2.2. Preparation of CEO nanoemulsions

The ratio of CEO to Tween80 (T80) was selected as 1:0, 1:1, 1:2, 1:4. The amount of CEO was adjusted to 125 mg/10 mL NE. To prepare CEO NEs, calculated amounts of T80 were added to water and vortexed for 2 min. Then CEO was added and vortexed again for 2 minutes. Finally, ultrasonication (US) was performed for 0, 1, 5, 10 and 20 min using an Omni Ruptor 400 (Omni International, Inc, USA). For this purpose, a stepped micro processing tip model OR-T156 (diameter: 3.8 mm, length: 25.6 cm) was used. NEs were ultrasonicated at 20 kHz, 50% power (400 Watt), 70% pulse for 0, 1, 5, 10 and 20 minutes. The notations used for CEO NEs are given in Table 1. Just vortexed samples were designated as 0 min ultrasonication.

Table 1. The notation used for preparing CEO NEs.

Oil Phase/Surfactant	Ratio	Notation				
		0 min	1 min	5 min	10 min	20 min
CEO/T80	1/0	W.0	W.1	W.5	W.10	W.20
	1/1	WT1.0	WT1.1	WT1.5	WT1.10	WT1.20
	1/2	WT2.0	WT2.1	WT2.5	WT2.10	WT2.20
	1/4	WT4.0	WT4.1	WT4.5	WT4.10	WT4.20

2.3. Characterizations

2.3.1. pH, electrical conductivity and surface tension of CEO nanoemulsions

The pH and electrical conductivity of CEO NEs were measured using a pH meter (Mettler Toledo SevenEasy pH-Meter) and conductivity meter (TPS, WP-Plus), respectively. Surface tension measurements were carried out using Attension Theta Flow Premium Contact Angle Optical Tensiometer (nanoScience Instruments Inc.) in air atmosphere and at room temperature. The surface tension of the raw materials and nanoemulsions were measured using the Pendant Drop method with 3-4 µL droplets at ambient temperature, 30% relative humidity and calculated using the Young/Laplace method. All measurements were performed in triplicate.

2.3.2. Ultra-violet visible spectroscopy analysis of CEO nanoemulsions

Turbidity of CEO NEs was determined by measuring the absorbance at 600 nm with a Varian Cary 300 UV-Vis spectrophotometer with/without dilution [33]. Ultrapure water was used as blank sample.

2.3.3. Dynamic light scattering (DLS) analysis of CEO nanoemulsions

To determine droplet size and Zeta potential of CEO NEs, DLS measurements were carried out at 25ºC Zetasizer Nano ZS (Malvern Panalytical Ltd, UK). It yields the mean droplet size as well as the polydispersity index (PDI), which represents the droplet size distribution. PDI values < 0.1 and >0.3 mean a very narrow and a very broad distribution, respectively [34]. Before measurements, 0,1 ml of nanoemulsions were diluted with 50 mL water and the pH was adjusted to 7,0 using buffer solution.

2.3.4. Statistical analysis for droplet size and Zeta potential of CEO nanoemulsions

The results obtained from Zetasizer Nano ZS measurements were evaluated in Design Expert®6.06 software by a statistical method using a general factorial design by determining surfactant amount, ultrasonication time and days as factors and droplet size (d50) and Zeta potential as response. ANOVA was applied to assess the statistical significance of the variations. The statistical significance of each factor was assessed by setting the significance level at $p \leq 0.05$. The contribution (%) of each factor on the respective response was also assessed.

2.3.5. Microscopy characterizations of CEO nanoemulsions

Scanning Electron Microscopy (SEM) and Transmission Electron Microscopy (TEM) characterizations were performed for evaluating morphology of the NEs generated. For the SEM, one drop 500 times diluted CEO NE was placed on silicon wafer. The samples were dried at 50°C overnight. Subsequently, the stubs were coated with platinum. An accelerating voltage of 2-5 kV was used using a Zeiss Supra 1555 VP field emission gun scanning electron microscope, secondary electron detector. For the TEM, a 3 µl of 500 times diluted CEO NE was placed on the 300 mesh copper grid and stained with ammonium molybdate aqueous solution (2 wt.%, pH:5,16) [35]. The stained samples were characterized at 200 kV by using JEOL 2100 LaB6 transmission electron microscope. (Figure 1). Sample preparation of nanoemulsions for TEM was as follows: A 300 mesh copper grid was taken from the grid holder (Figure 1.a) and it was held with tweezer on a Whatman filter paper carbon coated side face up (Figure

1.b). Using the side blot method, a 3 µL droplet of the sample was placed on the copper grid and waited for 1 min (Figure 1.c). The edge of the grid was touched to a sheet of filter paper to pull off the liquid through capillary action (Figure 1.d). Next, two 50 µL droplets of ultrapure water (Figure 1.e, designated as 1 and 2) and two 50 µL droplets of staining agent solution (2% ammonium molybdate pH:5,16) (Figure 1.e, designated as 3 and 4) were placed on a sheet of laboratory film (parafilm). The grid was touched gently to water droplet and lifted off a small droplet onto the surface of the grid (Figure 1.f). Then, the edge of the grid was touched to a sheet of filter paper to pull off the liquid through capillary action (Figure 1.g). This action was repeated twice. Afterwards, the grid was touched gently to the staining solution (Figure 1.h) and held for 10-15 sec. Then, the edge of the grid was touched to a sheet of filter paper to pull off the liquid through capillary action (Figure 1.i). This action was repeated twice as well. Finally, the TEM grid prepared with the sample was allowed to dry at ambient conditions and put it back to its holder before characterization (Figure 1.j).

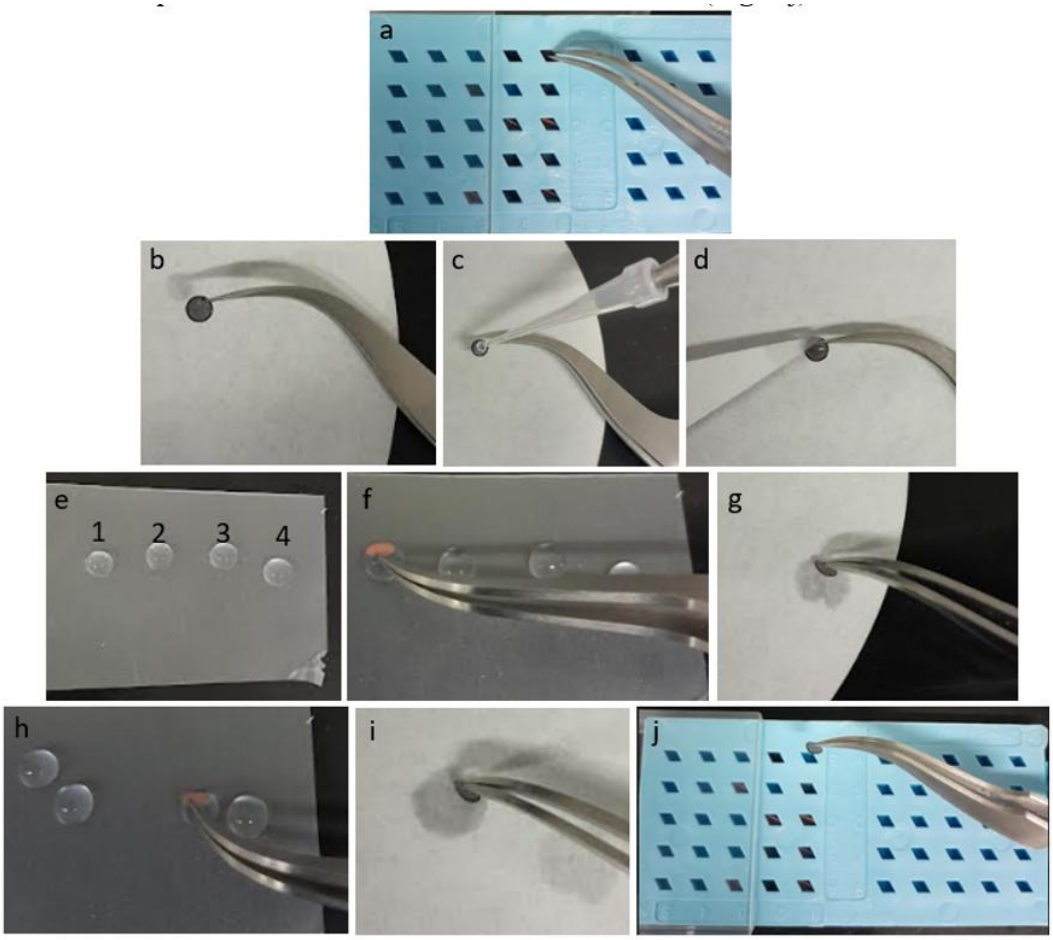

Figure 1. Sample preparation steps for TEM characterization. a. Taking a copper grid from the grid holder, b. Holding the grid with tweezer on a filter paper, c. Putting the sample droplet on the grid, d. Touching the edge of the grid to a sheet of filter paper, e. Putting droplets of ultrapure water (#1 and #2) and droplets of staining agent solution (#3 and #4) on a sheet of laboratory film (parafilm), f. Touching the grid to water droplet, g. Touching the edge of the grid to a sheet of filter paper, h. Touching the grid to the staining solution, i. Touching the edge of the grid to a sheet of filter paper, j. Putting the dried grid back to its holder.

3. Results

3.1. pH, electrical conductivity, and surface tension of CEO nanoemulsions

The results for pH, electrical conductivity and surface tension of the CEO NEs are given in Table 2. Water has a pH of 5.53±0.02. Regardless of the ultrasonication time, the surfactant-free CEO NEs showed almost identical pH values ranging from 6.20±0.02 to 6.32±0.01. Apparently, addition of CEO increased the pH value slightly. All other NEs containing different amounts of T80 led to further increase of the pH due to surfactant. However, the pH values were nearly the same, changing between 7.20±0.02 and 7.26±0.03.

The electrical conductivity of the water used was found to be 0.055 µS/cm. CEO NEs prepared without surfactant resulted in increased conductivity values with an increase in ultrasonication time. (17.2±1.2 µS/cm for W.0 and 27.1±1.6 µS/cm for W.20). Incorporation of the surfactant (WT1: NEs with 1/1 CEO/T80) resulted in further

increase of the conductivity values (29.1±2.1 µS/cm for WT1.0 and 34.0±1.3 µS/cm for WT1.20). Furthermore, conductivity was improved by increasing the T80 amount. According to these results, addition of T80 increased the electrical conductivity of the CEO NEs prepared. Nonetheless, the values are generally low, varying between 34.1±3.1 and 39.7±3.1 µS/cm.

Water exhibits a high surface tension value of 71.26±0.24 mN/m. In contrast, the neat T80 and the neat CEO exhibited substantially lower surface tension values of 31.68±0.05 and 27.61±0.32 mN/m, respectively. Furthermore, CEO NEs prepared exclusively using CEO yielded surface tension values ranging from 43.19±0.94 mN/m (W.0) to 49.83±0.13 mN/m (W.20). The incorporation of the T80 led to a further decline in surface tension values. However, the values didn't change depending on the ultrasonication time (39.45±0.15 mN/m for WT1.0 and 39.72±0.14 mN/m for WT1.20).

Table 2. pH, electrical conductivity, and surface tension of CEO NEs.

Notation	pH	Electrical Conductivity (μScm^{-1})	Surface Tension (mNm^{-1})
W.0	6.30±0.01	17.2±1.2	43.19±0.94
W.1	6.32±0.02	19.1±2.0	46.61±0.60
W.5	6.20±0.02	23.7±0.9	47.01±0.89
W.10	6.26±0.03	25.0±0.5	47.99±0.23
W.20	6.32±0.01	27.1±1.6	49.83±0.13
WT1.0	7.26±0.02	29.1±2.1	39.45±0.15
WT1.1	7.20±0.02	32.7±3.0	39.05±0.35
WT1.5	7.26±0.03	34.3±0.1	38.27±0.16
WT1.10	7.20±0.02	33.2±0.5	38.33±0.09
WT1.20	7.26±0.03	34.0±1.3	39.72±0.14
WT2.0	7.22±0.04	34.1±3.1	38.60±0.10
WT2.1	7.27±0.02	35.7±2.0	38.81±0.16
WT2.5	7.31±0.01	36.1±2.9	39.05±0.21
WT2.10	7.22±0.02	36.4±1.5	39.53±0.17
WT2.20	7.28±0.05	35.9±2.3	39.84±0.22
WT4.0	7.38±0.02	37.4±3.0	39.64±0.08
WT4.1	7.30±0.04	37.7±1.1	40.09±0.14
WT4.5	7.19±0.16	38.1±2.8	40.18±0.09
WT4.10	7.21±0.07	37.2±4.5	40.45±0.16
WT4.20	7.31±0.03	39.7±3.1	40.02±0.17

3.2. Optical transparency of CEO nanoemulsions

Visual images were taken and transparency measurements were performed in freshly prepared (0th day) and aged (42nd day) CEO NEs (Figure 2). The CEO NE prepared in the absence of US and T80 (W.0) delivered a transparent solution. Just vortexing without ultrasonication might have led to a microphase separation of oil and water which cannot be visible to the naked eye. On the other hand, independent of ultrasonication time, all CEO NEs had a blurry appearance.

Considering the NEs prepared by using surfactant delivered different results. An increase in both T80 concentration and ultrasonication time resulted in an appreciable color change in the emulsions from cloudy to clear appearance. The sample with CEO/T80 ratio of 1/1 (WT1) was slightly blurry before ultrasonication. Only 1-minute US (WT1.1) led to a totally blurry appearance. However, increasing the US time improved the transparency gradually. A ultrasonication time of 10 min (WT1.10) delivered a fully transparent solution. Increasing the time to 20 min made the solution slightly blurry again. The samples with other oil-to-surfactant ratios (1/2 (WT2) and 1/4 (WT4)) delivered the same results. Increasing the surfactant amount to 1/4 only changed the appearance of the 1-minute ultrasonicated sample (WT4.1) more transparent comparatively.

Considering the visual images together with absorbance values at 600 nm, following results were obtained: The samples prepared with CEO/T80 ratio of 1/4 and ultrasonicated delivered the most transparent solutions (0.1621 for 5 min US (WT4.5), 0,0872 for 10 min US (WT4.10), and 0,0000 for 20 min US (WT4.20)). Some ultrasonicated samples with CEO/T80 ratios of 1/1 and 1/2 also depicted quite close values (0,0250 for WT1.10, 0,0238 for WT2.10). Considering the same formulations after 42 days, all of them were only slightly blurrier than the freshly prepared ones. They delivered nearly the same results.

3.3. Statistical analysis for droplet size of CEO nanoemulsions

Before statistical evaluation of the results, droplet size, polydispersity index (PdI), and Zeta potential values are given in Table 3, Table 4, and Table 5, respectively.

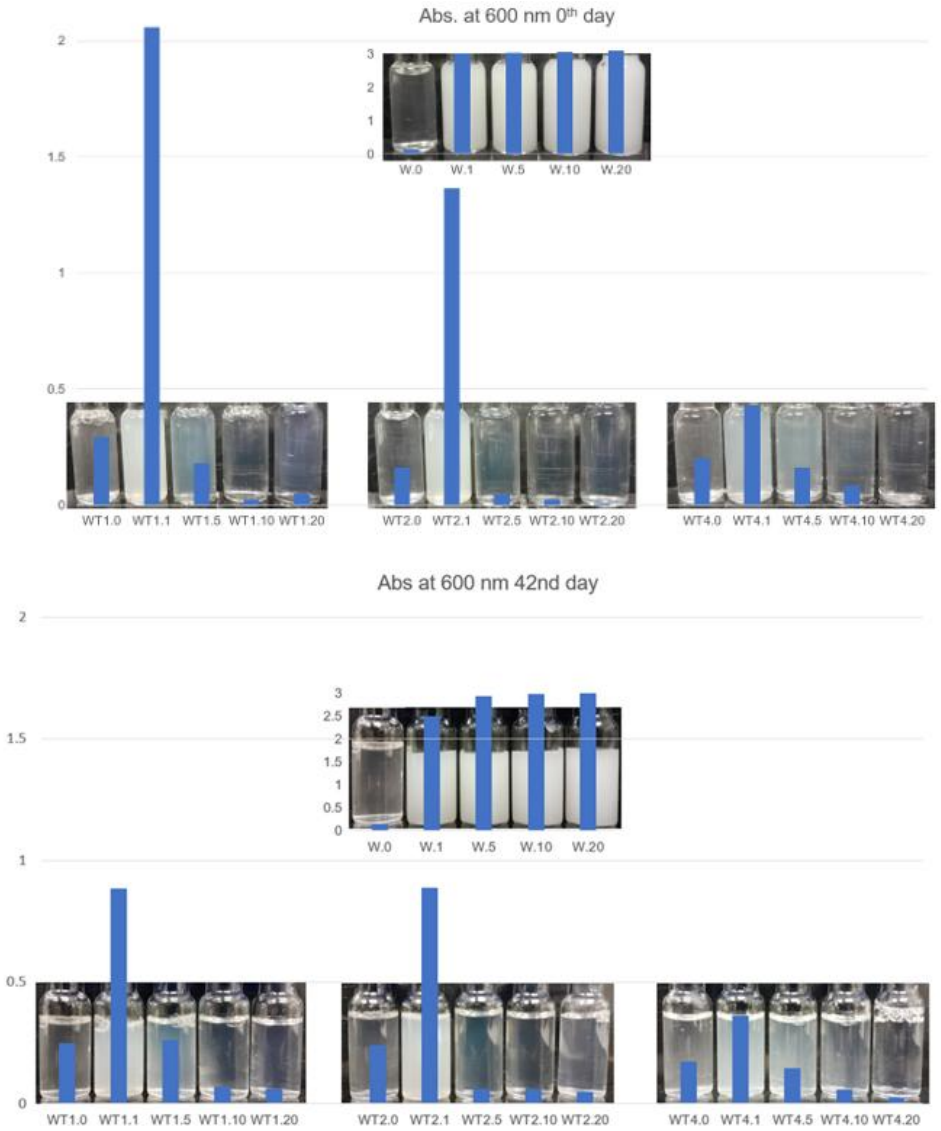

Figure 2. Physical appearance and turbidity values of freshly prepared (0th day) and aged (42nd day) CEO NEs at 600 nm depending on T80 amount.

Table 3. Droplet sizes of CEO NEs.

Notation	0 day		7 day		14 days		28 days		42 days	
	Z-Aver. (nm)	STD Dev.	Z-Aver. (nm)	STD Dev.	Z-Aver. (nm)	STD Dev.	Z-Aver. (nm)	STD Dev.	Z-Aver. (nm)	STD Dev.
W.0	376	67	648	26	563	34	865	12	847	81
W.1	299	7	288	7	303	1	386	41	316	6
W.5	326	1	356	4	306	8	359	51	324	3
W.10	289	8	390	6	308	13	324	1	378	46
W.20	258	12	315	6	396	2	364	37	376	16
WT1.0	259	15	213	78	250	11	340	39	495	15
WT1.1	221	14	214	18	299	15	357	32	360	11
WT1.5	100	43	110	8	140	2	170	39	283	46
WT1.10	65	2	48	1	131	4	190	8	232	46
WT1.20	229	101	246	43	395	8	338	40	371	33
WT2.0	192	15	248	26	139	25	207	2	278	17
WT2.1	175	2	192	5	194	7	279	4	241	50
WT2.5	53	3	63	0	97	4	191	6	201	22
WT2.10	51	3	71	33	51	4	128	28	126	27
WT2.20	39	3	33	8	79	0	100	47	75	6
WT4.0	157	18	78	2	212	17	219	71	169	16
WT4.1	243	6	270	22	276	33	309	54	287	12
WT4.5	238	4	205	17	213	18	207	22	241	5
WT4.10	50	5	60	2	52	8	244	42	235	1
WT4.20	26	3	22	4	30	6	84	3	63	10

Table 4. PdI values of CEO NEs.

Notation	0 day		7 days		14 days		28 days		42 days	
	PdI	STD Dev.	PdI	STD Dev.	PdI	STD Dev.	PdI	STD Dev.	PdI	STD Dev.
W.0	0.428	0.063	0.625	0.051	0.530	0.029	0.787	0.031	0.729	0.016
W.1	0.405	0.041	0.439	0.010	0.479	0.056	0.411	0.007	0.495	0.001
W.5	0.393	0.037	0.401	0.016	0.508	0.034	0.594	0.031	0.46	0.045
W.10	0.363	0.016	0.479	0.090	0.420	0.006	0.472	0.059	0.465	0.045
W.20	0.308	0.059	0.360	0.030	0.485	0.003	0.533	0.016	0.369	0.014
WT1.0	0.438	0.021	0.472	0.272	0.336	0.016	0.353	0.012	0.469	0.008
WT1.1	0.391	0.056	0.424	0.016	0.396	0.073	0.372	0.017	0.388	0.022
WT1.5	0.323	0.081	0.401	0.054	0.214	0.001	0.389	0.026	0.387	0.043
WT1.10	0.456	0.001	0.505	0.032	0.272	0.023	0.361	0.011	0.306	0.009
WT1.20	0.442	0.082	0.497	0.001	0.403	0.197	0.246	0.084	0.374	0.146
WT2.0	0.734	0.121	0.528	0.115	0.534	0.161	0.341	0.020	0.463	0.024
WT2.1	0.413	0.005	0.472	0.015	0.520	0.102	0.488	0.074	0.471	0.129
WT2.5	0.381	0.017	0.346	0.007	0.577	0.142	0.358	0.021	0.237	0.046
WT2.10	0.304	0.406	0.307	0.093	0.533	0.032	0.381	0.040	0.403	0.128
WT2.20	0.466	0.028	0.524	0.255	0.545	0.009	0.398	0.017	0.696	0.001
WT4.0	0.724	0.032	0.729	0.066	0.771	0.144	0.547	0.001	0.302	0.083
WT4.1	0.601	0.016	0.653	0.011	0.652	0.003	0.403	0.038	0.334	0.011
WT4.5	0.521	0.023	0.621	0.056	0.607	0.091	0.495	0.096	0.371	0.039
WT4.10	0.501	0.120	0.586	0.018	0.521	0.154	0.345	0.051	0.391	0.007
WT4.20	0.577	0.182	0.677	0.026	0.573	0.033	0.498	0.056	0.770	0.090

Table 5. Zeta potential values of CEO NEs.

Notation	0 day		7 day		14 days		28 days		42 days	
	Zeta (mV)	STD Dev.	Zeta (mV)	STD Dev.	Zeta (mV)	STD Dev.	Zeta (mV)	STD Dev.	Zeta (mV)	STD Dev.
W.0	-33.5	2.1	-33.1	2.1	-38.5	0.2	-35.2	3.5	-31	4.7
W.1	-39.8	0.4	-31.1	0.4	-35.9	1	-35.2	0.4	-29.6	1.5
W.5	-34.7	0.2	-38.1	0.7	-35.9	1.2	-30	1.7	-32.8	1.1
W.10	-40	0.8	-43.8	1.9	-39.7	0.4	-33.4	0.4	-32.9	1.1
W.20	-42.3	0.6	-37.8	0.3	-37.3	0.6	-34	0.3	-35	1
WT1.0	-41.1	1.1	-34.2	2.1	-28.8	3.7	-19.5	9.7	-11.4	2.5
WT1.1	-37.6	0.5	-37.1	3.5	-25.6	0.5	-19.9	7.5	-18.5	6.5
WT1.5	-36.3	5.5	-39.6	3.6	-33.4	3.9	-18.1	6.5	-18.6	0.4
WT1.10	-33.6	3.4	-40.3	1.8	-29.6	0.5	-19	1.1	-21.7	2.6
WT1.20	-36	3.3	-38.7	4.2	-30.1	1.5	-16.8	0.6	-18.9	1.4
WT2.0	-36.9	1.8	-34.7	2.6	-31.2	0.8	-25	9	-21.9	6.5
WT2.1	-41.5	1	39.1	2.1	-32	0.9	-24	2.7	-21	0.1
WT2.5	-37	2.5	-36.1	2.6	-30.3	1.2	-20.2	3.6	-21.6	0.3
WT2.10	-37.7	3.5	-37.4	1.6	-31.4	2.5	-26.3	2.8	-26.7	1.5
WT2.20	-34.4	2.6	-37.2	2.2	-33.6	3.8	-25.5	3.5	-24.5	2.5
WT4.0	-35.9	0.3	-37.9	5.5	-32.6	8.5	-30.3	0.5	-19	4.9
WT4.1	-34.1	3.3	-38.5	6.8	-32.5	5.2	-23	2.3	-20	1.7
WT4.5	-33.6	7.3	-36.4	4	-34.3	7.4	-23.8	1.6	-21.2	7
WT4.10	-38.9	1.1	-39.5	2.7	-31.4	1.9	-25.5	1.1	-18.3	1.6
WT4.20	-35.6	2.1	-37.5	3	-28.2	5.5	-20.2	1.8	-15	2.2

To reveal optimum emulsification conditions, droplet size (d_{50}) of CEO NEs were evaluated statistically. The statistical analysis was started with model selection. Following the entry of the droplet size data into the Design Expert® 6.06 software, the model with the largest sum of squares, F-values, the smallest p-value (Prob > F), the largest R-squared and the smallest PRESS (Predicted Errors Sum of Squares) can be recommended. The cubic model that mostly satisfied the mentioned conditions was suggested for the analysis of droplet sizes, although linear model and quadratic model had the largest F-value than the cubic model.

To judge the statistical significance of the variations, ANOVA was applied by using general factorial design considering surfactant amount, ultrasonication time, and days as input variables and droplet size as response variable. The results are shown in Table 6, which will be evaluated in Section 4. Discussion and Conclusion.

Table 6. ANOVA table for droplet size of CEO NEs.

Source	Sum of Sq.	Contribution %	DF	Mean Sq.	F-value	Prob > F	
Model	1069597	89,8626	27	39614,7	21,99701	< 0.0001	**significant**
A	561207,1	47,15004	3	187069	103,8746	< 0.0001	**significant**
B	101056,9	8,490337	1	101056,9	56,11427	< 0.0001	**significant**
C	116720,9	9,806355	1	116720,9	64,81209	< 0.0001	**significant**
B^2	66983,08	5,62761	1	66983,08	37,19396	< 0.0001	**significant**
C^2	1109,082	0,09318	1	1109,082	0,615845	0.4354	Not significant
AB	103536,2	8,698634	3	34512,06	19,16365	< 0.0001	**significant**
AC	37089,45	3,116085	3	12363,15	6,864936	0.0004	**significant**
BC	237,0451	0,019915	1	237,0451	0,131625	0.7179	Not significant
B^3	1376,991	0,115688	1	1376,991	0,764607	0.3850	Not significant
C^3	2854,512	0,239823	1	2854,512	1,585036	0.2124	Not significant
AB^2	106315,4	8,932132	3	35438,47	19,67806	< 0.0001	**significant**
AC^2	1163,805	0,097778	3	387,935	0,21541	0.8854	Not significant
B^2C	4929,818	0,414181	1	4929,818	2,7374	0.1027	Not significant
BC^2	4377,673	0,367792	1	4377,673	2,430808	0.1237	Not significant
ABC	9767,088	0,820586	3	3255,696	1,807803	0.1541	Not significant
Residual	120661,2	10,1374	67	1800,913			
Cor.Total	1190258	100	94				

The regression equations according to surfactant amount emerged from the developed model are shown below.

No Surfactant

Average Droplet Size = 337,2729 - 0,12733xB - 3,27491xC - 0,70267xB^2 + 0,173656xC^2 + 0,588343xBxC + 0,029597xB^3 - 0,00281xC^3 - 0,01166xB^2xC - 0,00527xBxC^2

Surfactant Amount T1

Average Droplet Size = 244,4407 - 36,3297xB - 0,04795xC + 1,265108xB^2 + 0,222846xC^2 + 0,364877xBxC + 0,029597xB^3 - 0,00281xC^3 - 0,01166xB^2xC - 0,00527xBxC^2

Surfactant Amount T2

Average Droplet Size = 191,4485 - 19,8582xB -1,71995xC + 0,008023xB^2 + 0,202649xC^2 + 0,412459xBxC + 0,029597xB^3 - 0,00281xC^3 - 0,01166xB^2xC - 0,00527xBxC^2

Surfactant Amount T4

Average Droplet Size = 235,875 - 9,54106xB - 2,26773xC - 0,751xB^2 + 0,178067xC^2 + 0,552195xBxC + 0,029597xB^3 - 0,00281xC^3 - 0,01166xB^2xC - 0,00527xBxC^2

The regression contour plots are demonstrated in Figure 3 according to surfactant amount by determining the regression equations. Here x-axis represents ultrasonication time, y-axis shows the days, contours show the droplet size of CEO NEs. The results of the contour plots will be evaluated and discussed in Section 4. Discussion and Conclusion.

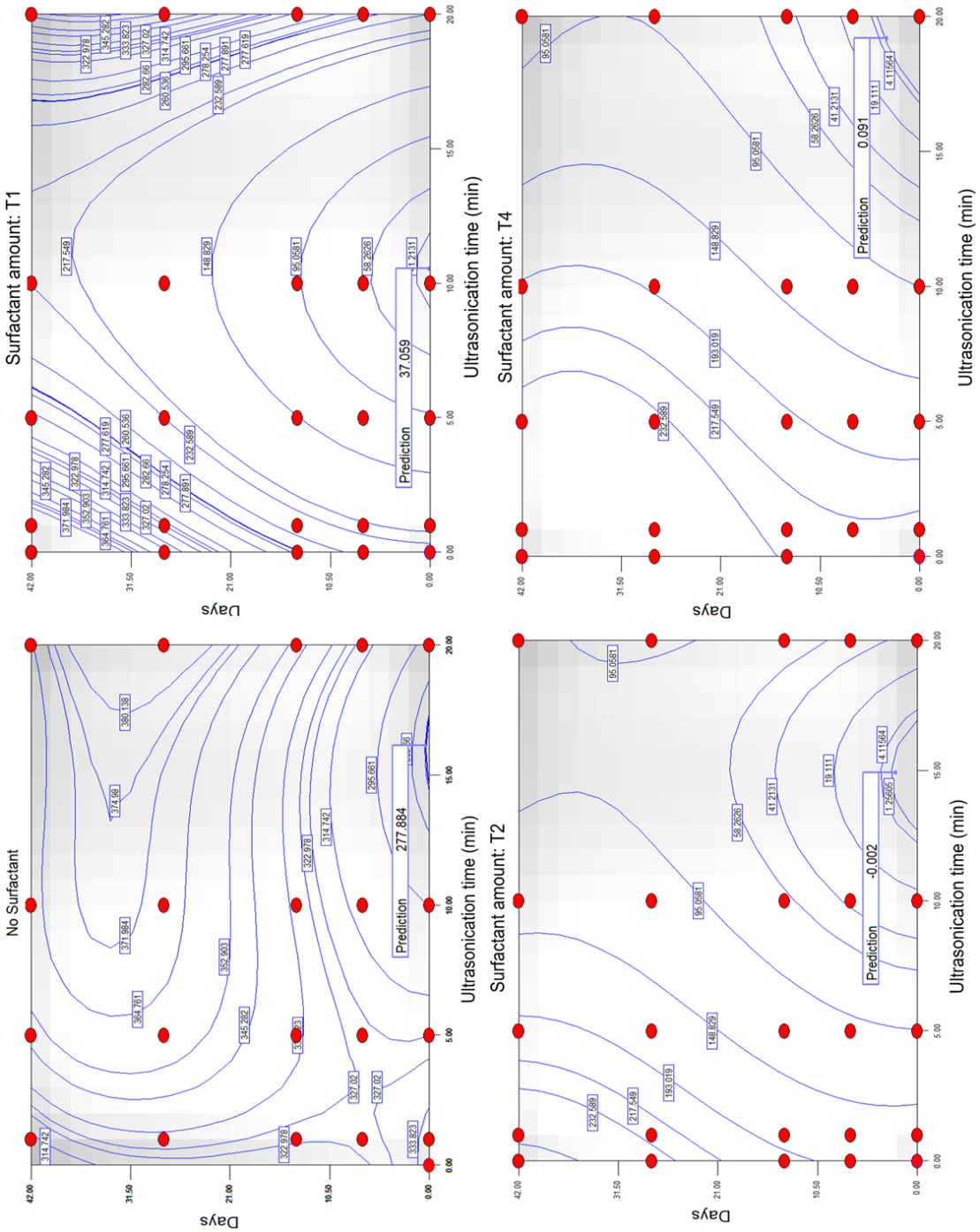

Figure 3. Regression contour plots for droplet size of CEO NEs without surfactant and with surfactant (T1, T2, and T4).

3.4. Morphology of CEO nanoemulsions

The SEM images are illustrated in Figure 4. In order to facilitate a comparison between the results of SEM with those of DLS measurements, the droplet sizes observed in the SEM images were subject to a coarse quantitative analysis based on visual inspection. The results are presented in Table 7, alongside the DLS results obtained from the optimised processing conditions. The results obtained from the SEM characterisation appear to be analogous to those obtained from the DLS measurements.

Laborious sample preparation process, time-consuming measurements, and limited availability of TEM restricts its use. Therefore, only the CEO NE prepared using a CEO/T80 of 1/1 and ultrasonicated for 10 min (WT1.10) was used for the TEM characterization (Figure 5). According to the TEM image, droplet size of ca. 50-150 nm was observed, which was in accordance with the DLS results (65±2 nm).

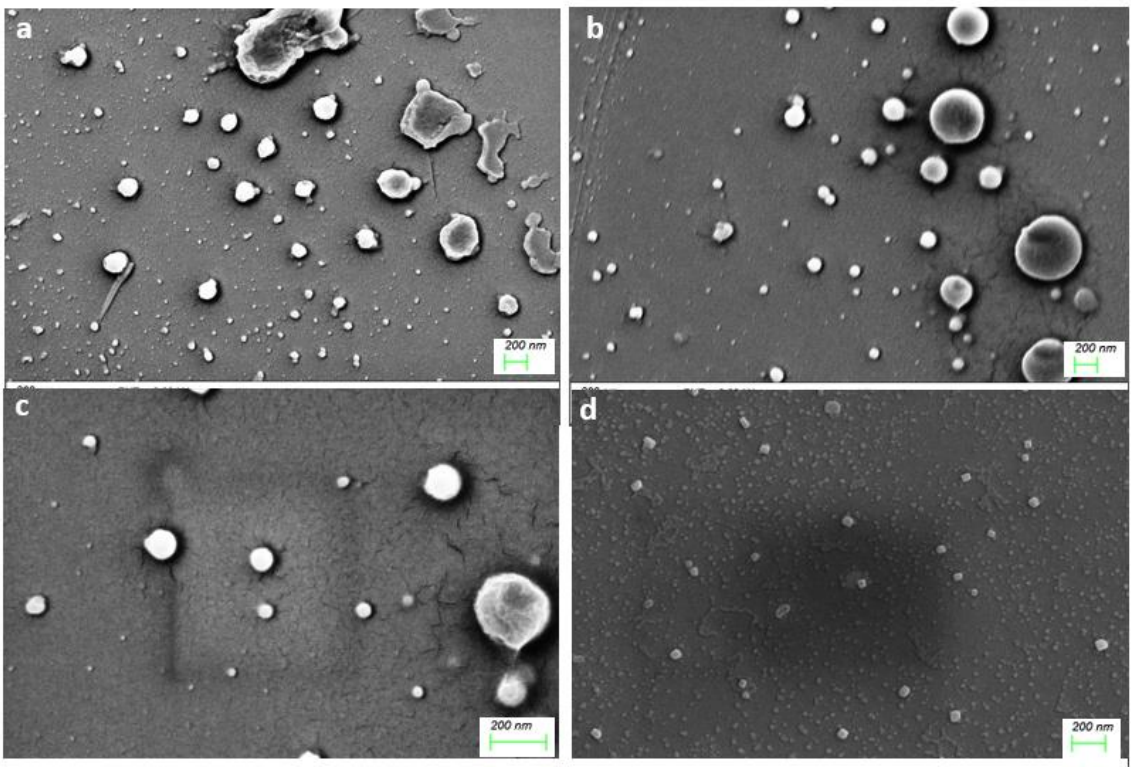

Figure 4. SEM images of CEO NEs (a: W.0, b: W.10, c; WT1.0, d: WT1.10).

Table 7. Rough comparison of droplet sizes of CEO NEs obtained from SEM and DLS.

Notation	Droplet Size (nm)	
	SEM	DLS
W.0	200-300	376±67
W.10	100-300	289±8
WT1.0	80-300	259±15
WT1.10	<100	65±2

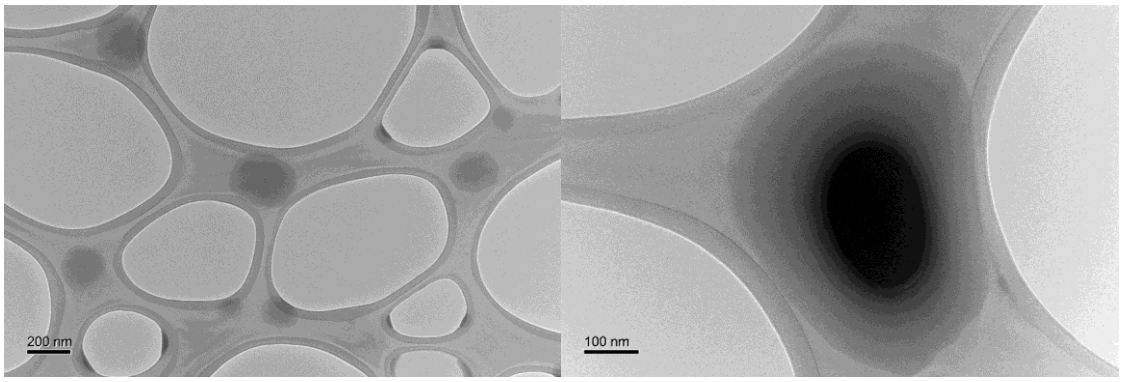

Figure 5. TEM image of the CEO NE (WT1.10).

4. Discussion and Conclusion

The purpose of this study was to reveal optimum processing conditions for chasteberry essential oil nanoemulsions. Considering visual inspection and UV-Vis evaluation of the CBO NEs, it can be said that the distinctive color change observed during the generation of emulsion could be attributed to the Rayleigh scattering effect due to the formation of nano-sized droplets [36]. Accordingly, transparency of the emulsions might be an indication of the presence of nano-sized droplets. Even the aged NEs showed the same result meaning that they kept their stability even after 42 days. The formation was a non-spontaneous process due to its positive Gibbs free energy. However, surfactant/emulsifier could reduce this positive free energy, thereby improving its spontaneous character and the stability of the NEs [6,37].

Statistical evaluation of droplet size values of CBO NEs delivered the following results: According to Table 6, the model developed explains 89,86% of the droplet sizes with these data. In addition, surfactant amount (A), ultrasonication time (B), and days (C) are significant parameters on the droplet size. However, the most significant

factor on droplet size is the surfactant amount (A) with 47,15% contribution. ultrasonication time (B+B2) and the day (C+C2) have 14,12% and 9,9% contributions on the droplet size, respectively.

When all contour plots in Figure 3 are considered, it can be concluded that the minimum droplet size (Prediction: 37.059 nm) can be achieved by determining days:0 and ultrasonication time as 10.55 min by using T1 (CEO/T80: 1/1). It is astonishing to note that the optical transparency values literally supported the statistical analysis results of the droplet size. Accordingly, a CEO/T80 of 1/1 employing an US time of 10 min (WT1.10) delivered the most transparent and the smallest droplet sizes.

Considering all results, following conclusions can be drawn: Droplet sizes of chasteberry essential oil nanoemulsions increased with increasing aging time. The presence of a very broad droplet size distribution in all NEs indicates that ultrasonication alone is inadequate for achieving a narrow distribution. All NEs exhibited relatively high Zeta potential absolute values (>30). Despite the decrease in Zeta potential values over time, they were found to be generally stable, even in the long term.

This study showed that chasteberry essential oil containing nanoemulsions could be prepared by employing a simple ultrasonication using only water and a surfactant. Statistical analyses results of the droplet size values delivered complementary results in addition to physical appearance and turbidity measurement results. The prepared nanoemulsions were also shown to be stable in the long-term and could be used in cream and/or gel formulations for women's health, where storage stability is important. As a future study, chasteberry essential oil will be provided from different sources and related formulations are planned to prepare and compare their efficacy.

Acknowledgment

This work was supported by the TUBITAK 2219 International Post-doctoral Research Fellowship Program for Turkish Citizens [grant number 1059B191900929]. Prof. Minoo Naebe from Deakin University, Australia was greatly acknowledged for her kind support.

References

[1] Christaki, E., Bonos, E., Giannenas, I., Florou-Paneri, P. 2012. Aromatic plants as a source of bioactive compounds. Agriculture, 2(3), 228–243.

[2] Bakry, A.M., Abbas, S., Ali, B., Majeed, H., Abouelwafa, M.Y. et al. 2016. Microencapsulation of oils: a comprehensive review of benefits, techniques, and applications, Comprehensive Reviews in Food Science and Food Safety, 15 (1), 143-182.

[3] Turek, C., Stintzing, F.C. 2013. Stability of essential oils: a review, Comprehensive Reviews in Food Science and Food Safety, 12 (1), 40-53.

[4] Acosta, E. 2009. Bioavailability of nanoparticles in nutrient and nutraceutical delivery, Current Opinion in Colloid and Interface Science, 14(1), 3-15.

[5] McClements, D.J., Decker, E.A., Weiss, H. 2007. Emulsion-based delivery systems for lipophilic bioactive components, Journal of Food Science, 72(8), R109-R124.

[6] Tadros, T., Izquierdo, P., Esquena, J., Solans, C. 2004. Formation and stability of nano-emulsions, Advances in Colloid and Interface Science, 108, 303-318.

[7] Taha, A., Ahmed, E., Ismaiel, A., Ashokkumar, M., Xu, X. et al. 2020. Ultrasonic emulsification: An overview on the preparation of different emulsifiers-stabilized emulsions, Trends in Food Science & Technology, 105, 363-377.

[8] Chung, C., Sher, A., Rousset, P., Decker, E.A., McClements, D.J. 2017. Formulation of food emulsions using natural emulsifiers: Utilization of quillaja saponin and soy lecithin to fabricate liquid coffee whiteners, Journal of Food Engineering, 209: 1-11.

[9] van Nieuwenhuyzen, W. 2015. Production and utilization of natural phospholipids. Polar Lipids: Biology, Chemistry, and Technology. The Netherlands: AOCS Press.

[10] Kralova, I., Sjöblom, J. 2009. Surfactants used in food industry: a review, Journal of Dispersion Science and Technology, 30, 1363-1383.

[11] Leser, M.E., Sagalowicz, L., Michel, M., Watzke, H.J. 2006. Self-assembly of polar food lipids, Advances in Colloid and Interface Science, 123-126, 125–136.

[12] Ziani, K., Chang, Y., McLandsborough, L., McClements, D.J. 2011. Influence of surfactant charge on antimicrobial efficacy of surfactant-stabilized thyme oil nanoemulsions, Journal of Agricultural and Food Chemistry, 59, 6247-6625.

[13] Hait, S.K., Moulik, S.P. 2001. Determination of critical micelle concentration (CMC) of nonionic surfactants by donor-acceptor interaction with lodine and correlation of CMC with hydrophile-lipophile balance and other parameters of the surfactants, Journal of Surfactants and Detergents, 4, 303–309.

[14] Anton, N., Vandamme, T.F. 2011. Nano-emulsions and micro-emulsions: clarifications of the critical differences, Pharmaceutical Research, 28, 978-985.

[15] Gupta, A., Eral, H.B., Hatton, T.A., Doyle, P.S. 2016. Nanoemulsions: formation, properties and applications. Soft Matter, 12(11), 2826-2841.

[16] McClements, D.J. 2012. Nanoemulsions versus microemulsions: terminology, differences, and similarities. Soft Matter, 8(6), 1719-1729.

[17] Saifullah, M., Ahsan, A., Shishir, M.R.I. 2016. "Production, stability and application of micro- and nanoemulsion in food production and the food processing industry," in Nanotechnology in the Agri-Food Industry, Emulsions, ed A. M. Grumezescu (Cambridge, MA: Academic Press), 405–442.

[18] Patel, R.B., Patel, M.R., Thakore, S.D., Patel, B.G. 2017. Chapter 17 - Nanoemulsion as a Valuable Nanostructure Platform for Pharmaceutical Drug Delivery, Editor(s): Alexandru Mihai Grumezescu. Nano- and Microscale Drug Delivery Systems, Elsevier, 321-341.

[19] Tunç, E.N., Kaplan, A.B.U., Kılınboz, Y.F., Çetin, M. 2023. Nanoemulsion formulation containing carbamazepine and levetiracetam: Development and in vitro characterization, İstanbul Journal of Pharmacy, 53(2), 133-139.

[20] Bouchemal, K., Briançon, S., Perrier, E., Fessi, H. 2004. Nano-emulsion formulation using spontaneous emulsification: solvent, oil and surfactant optimisation, International Journal of Pharmaceutics, 280, 241-251.

[21] Chemat, F., Zill-E-Huma, Khan, M.K. 2011. Applications of ultrasound in food technology: Processing, preservation and extraction, Ultrasonics Sonochemistry, 18 (4), 813-835.

[22] Li, W., Leong, T.S.H., Ashokkumar, M., Martin, G.J.O. 2017. A study of the effectiveness and energy efficiency of ultrasonic emulsification, Physical Chemistry Chemical Physics, 20 (1), 86-96.

[23] Jafari, S.M., Assadpoor, E., He, Y., Bhandari, B. 2008. Re-coalescence of emulsion droplets during high-energy emulsification, Food Hydrocolloids, 22, 1191-1202.

[24] Cucheval, A., Chow, R.C.Y. 2008. A study on the emulsification of oil by power ultrasound, Ultrasonics Sonochemistry, 15(5), 916-920.

[25] Puglia, L.T., Lowry, J., Tamagno, G. 2023. Vitex agnus castus effects on hyperprolactinaemia, Frontiers in Endocrinology, 14, 1-9.

[26] Keikha, N., Shafaghat, M., Mousavi, S.M., Moudi, M., Keshavarzi, F. 2018. Antifungal effects of ethanolic and aqueous extracts of vitex agnus-castus against vaginal isolates of Candida albicans, Current Medical Mycology, 4(1), 1-5.

[27] Asdadi, A., Hassani, L.M.I., Chebli, B., Moutaj, R., Gharby, S. et al. 2014. Chemical composition and antifungal activity of vitex agnus-castus l. seeds oil growing in Morocco. J. Mater. Environ. Sci., 5(3), 823-830.

[28] Özen, İ., Demiryürek, O., Ceylan, A., Kaplan, A.B.U, Çetin, M. et al. 2024. Sustainable bio-sourced nanoemulsions: Pectin-based delivery systems for vitex essential oil and its therapeutic potentials. International Journal of Polymeric Materials and Polymeric Biomaterials, 1–13.

[29] Piazzini, V., Monteforte, E., Luceri, C., Bigagli, E., Bilia, A.R. et al. 2017. Nanoemulsion for improving solubility and permeability of Vitex agnus-castus extract: formulation and in vitro evaluation using PAMPA and Caco-2 approaches, Drug Delivery, 24(1), 380-390.

[30] Chinese Patent, J.W.P.D., CO, 2010. Vitex oil nanoemulsion and preparation method thereof, CN101773578A.

[31] Kassem, M.G.A., Ahmed, A.M.M., Abdel-Rahman, H.H., Moustafa, A.H.E. 2019. Use of Span 80 and Tween 80 for blending gasoline and alcohol in spark ignition engines, Energy Reports, 5, 221-230,

[32] Ahimsa Oils, 2023. Chaste Tree (Vitex) Oil, (Access Date: 10.04.2023).

[33] Nirmala, M.J., Durai, L., Gopakumar, V., Nagarajan, R. 2020. Preparation of celery essential oil-based nanoemulsion by ultrasonication and evaluation of its potential anticancer and antibacterial activity, International Journal of Nanomedicine, 15, 7651-7666.

[34] Scholz, P., Keck, C.M. 2015. Nanoemulsions produced by rotor–stator high speed stirring, International Journal of Pharmaceutics, 482 (1-2), 110-117.

[35] Salvia-Trujillo, L., Rojas-Graü, M.A., Soliva-Fortuny, R., Martín-Belloso, O. 2013. Effect of processing parameters on physicochemical characteristics of microfluidized lemongrass essential oil-alginate nanoemulsions, Food Hydrocolloids, 30, 401-407.

[36] Mason, T.G., Wilking, J.N., Meleson, K., Chang, C.B., Graves, S.M. 2006. Nanoemulsions: formation, structure, and physical properties, Journal of Physics: Condensed Matter, 18(41), R635.

[37] Hasani, F., Pezeshki, A., Hamishehkar, H. 2015. Effect of surfactant and oil type on size droplets of betacarotene-bearing nanoemulsions, International Journal of Current Microbiology Applied Sciences, 4(9), 146-155.